

Supporting Supplementary Information

Facile metal-free synthesis of pyrrolo[3,2-*b*]pyrrolyl-based conjugated microporous polymers for high-performance photocatalytic degradation of organic pollutants

Jing Han Wang, Chih-Ling Chang, Zhe Wei Zhang, Ahmed F. M. EL-Mahdy *

Department of Materials and Optoelectronic Science, National Sun Yat-Sen University,
Kaohsiung, 80424, Taiwan
E-mail: ahmedelmahdy@mail.nsysu.edu.tw

Experimental details

Materials

Chemicals and solvents were obtained from commercial sources and used as received. *p*-phenylenediamine (PDA), terephthalaldehyde (TPA), benzidine (BZI), and [1,1'-biphenyl]-4,4'-dicarbaldehyde (BID) were purchased from Alfa Aesar. Butane-2,3-dione was obtained from Sigma-Aldrich.

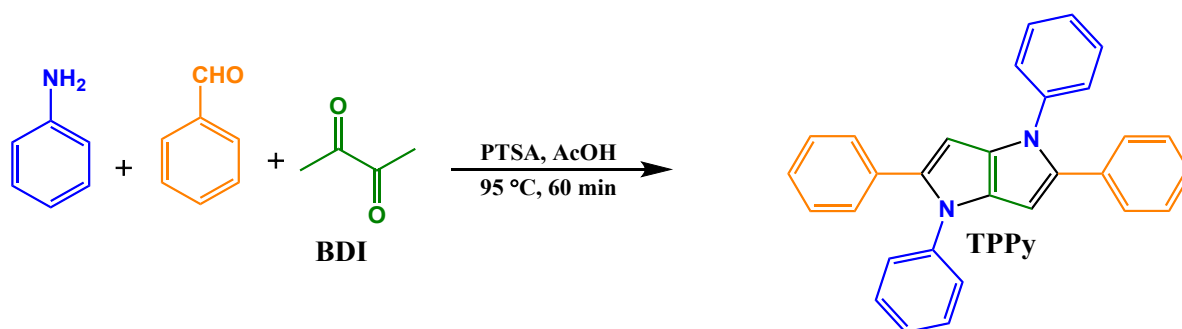
Characterizations

Fourier-transform infrared spectroscopy (FTIR) spectroscopy was recorded using a Bruker Tensor 27 FTIR spectrophotometer and the conventional KBr plate method; 32 scans were collected at a resolution of 4 cm⁻¹. Solid state nuclear magnetic resonance (SSNMR) spectroscopy was recorded using a Bruker Avance 400 NMR spectrometer and a Bruker magic-angle-spinning (MAS) probe, running 32,000 scans. Thermogravimetric analysis (TGA) was performed using a TA Q-50 analyzer under a flow of N₂. The samples were sealed in a Pt cell and heated from 40 to 700 °C at a heating rate of 20 °C min⁻¹ under N₂ at a flow rate of 50 mL min⁻¹. Nitrogen adsorption-desorption measurements were carried out using a BelSorp max instrument. Before measuring gas adsorption, the as-prepared samples (50 mg) were washed with anhydrous tetrahydrofuran for 24 hours using Soxhlet extraction. The solvent was filtered, and the samples were activated for 10 hours under pressure at 150 °C. The samples

were then used for gas adsorption-desorption measurements at 77 K from 0 to 1 atm. Their specific surface areas were calculated using the Brunauer-Emmett-Teller (BET) methodology. The pore distributions were calculated from the sorption data using the quenched solid state density functional theory. Field-emission scanning electron microscopy (FE-SEM) was conducted using a JEOL JSM-7610F scanning electron microscope. Samples were subjected to Pt sputtering for 100 s prior to observation. Transmission electron microscopy (TEM) was performed using a JEOL-2100 scanning electron microscope, operated at 200 kV. Samples for UV-Vis and fluorescence spectroscopy were dissolved in suitable organic solvents and placed in a small quartz cell ($0.2 \times 1.0 \times 4.5 \text{ cm}^3$). UV-Vis-NIR spectra were recorded at 25 °C using a Jasco V-570 spectrometer, with deionized water as the solvent.

Synthetic procedures

Synthesis of a model molecular analogue



Scheme S1. Synthesis of 1,2,4,5-tetraphenyl-1,4-dihydropyrrolo[3,2-*b*]pyrrole (TPPy).

In a 25-mL Schlenk storage tube, benzaldehyde (10 mmol, 1.06 g), aniline (10 mmol, 0.93 g), and *p*-toluenesulfonic acid (0.1 mmol, 19 mg) were dissolved in glacial acetic acid (20 mL). After the reaction temperature reach to 90 °C, β-diketone (5 mmol, 430.5 mg) was slowly added via syringe and the resulting mixture was stirred at 90 °C for 60 min. After cooling to room temperature, the precipitate filtered off and washed two times each with glacial acetic acid, water, methanol. The crude solid was purified by chromatography on silica gel using petroleum ether/dichloromethane as eluent. The solid was dried under vacuum at 80 °C overnight to afford a yellow powder for TPPy (50%). ¹H-NMR (500 MHz, DMSO-*d*₆, δ): 7.42 (dd, *J* = 10 Hz, 8H), 7.30-7.22 (m, 8 H), 7.18 (t, *J*=10 Hz, 4H), 6.45 (s, 2H); ¹³C-NMR (100 MHz, DMSO-*d*₆, δ): 140.33, 135.93, 133.78, 132.01, 130.14, 129.00, 128.24, 125.46, and 95.62 ppm.

Synthesis of Py-CMPS

In a 25-mL Schlenk storage tube, aryl aldehydes (4 mmol) (TPA = 536 mg, BID = 841 mg), aryl anilines (4 mmol) (PDA = 432 mg, BZI = 737 mg), and p-toluenesulfonic acid (0.4 mmol, 76 mg) were dissolved in glacial acetic acid (20 mL). After the reaction temperature reach to 90 °C, β -diketone (2 mmol, 172.2 mg) was slowly added via syringe and the resulting mixture was stirred at 90 °C for 60 min. After cooling to room temperature, the precipitate filtered off and washed two times each with glacial acetic acid, water, methanol, THF, and acetone. The solid was dried under vacuum at 120 °C overnight to afford a light-orange powder for Py-CMP-1 (85%) and orange powder for Py-CMP-2 (87%).

Spectral Profiles of TPPy

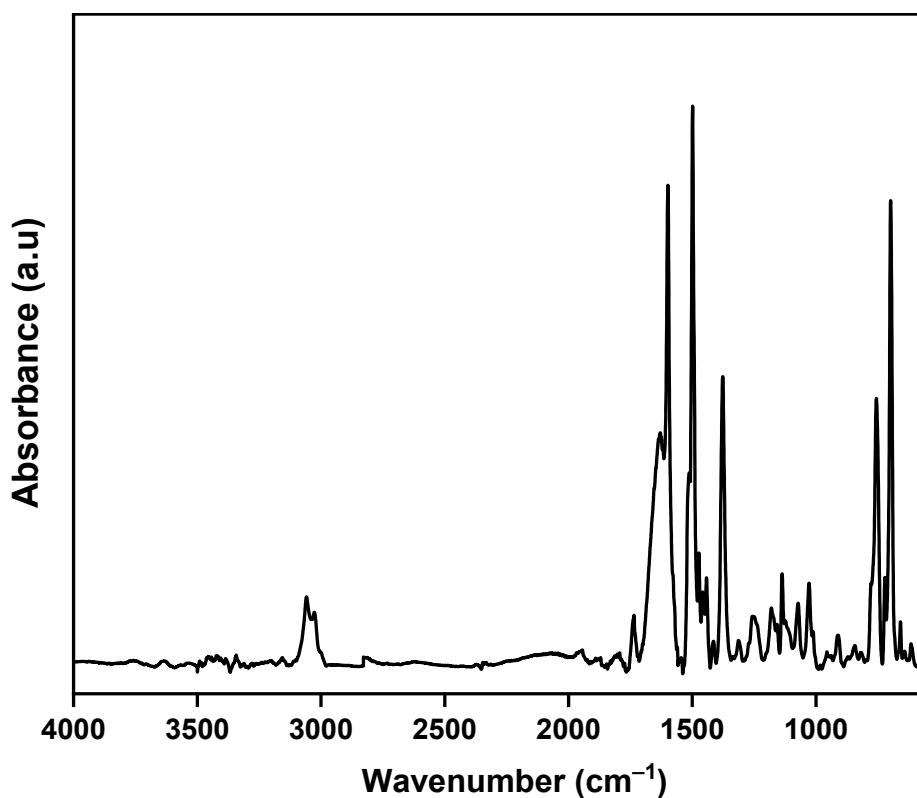


Figure S1. FTIR spectrum of TPPy.

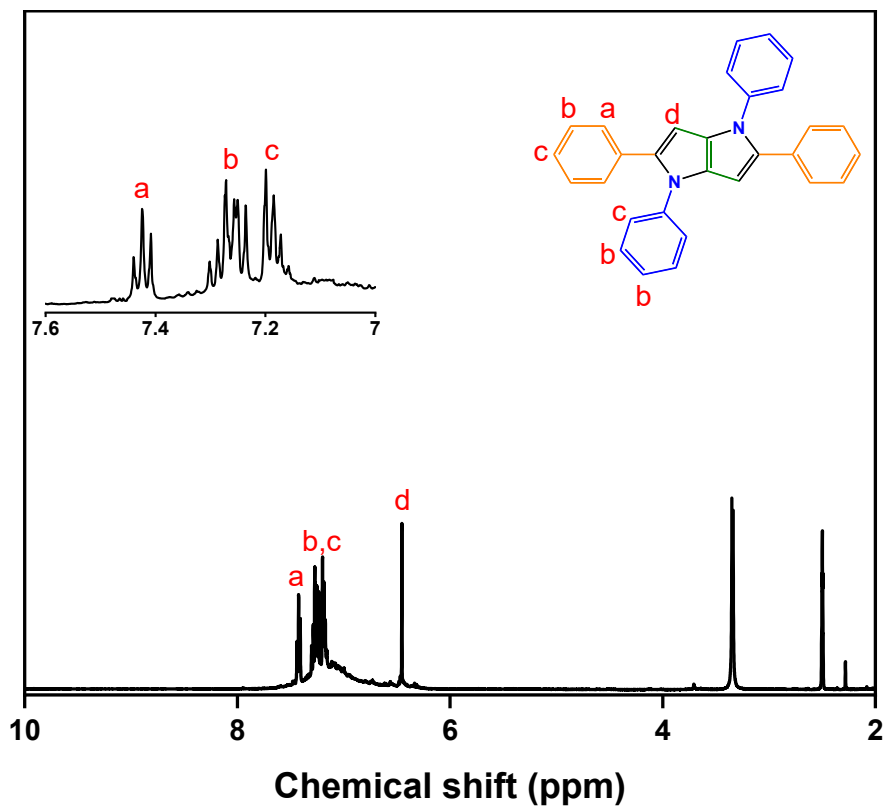


Figure S2. ^1H NMR spectrum of TPPy.

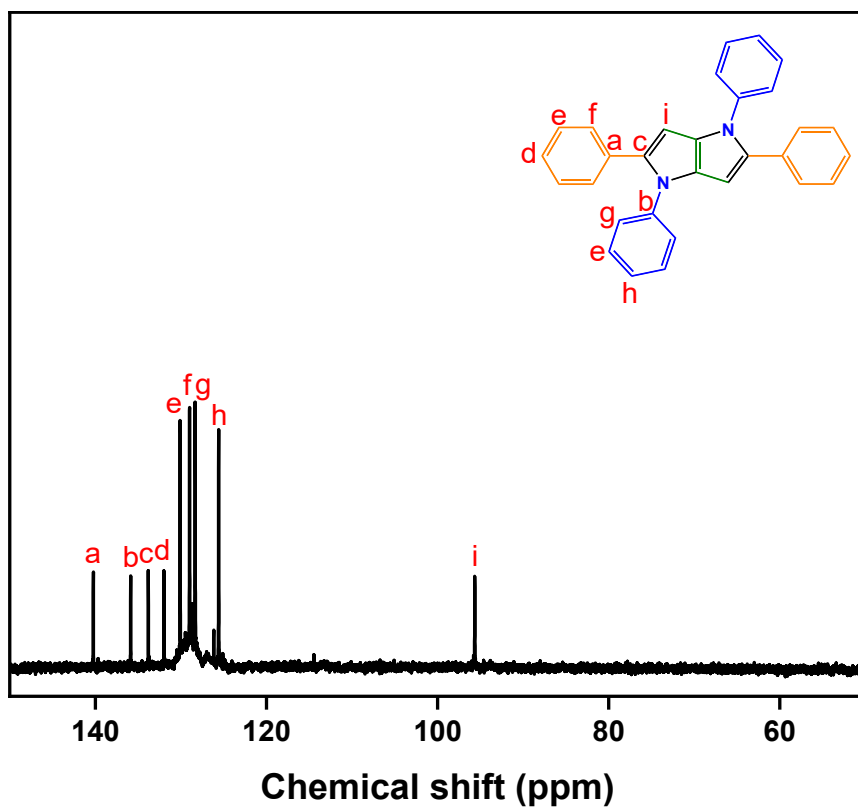
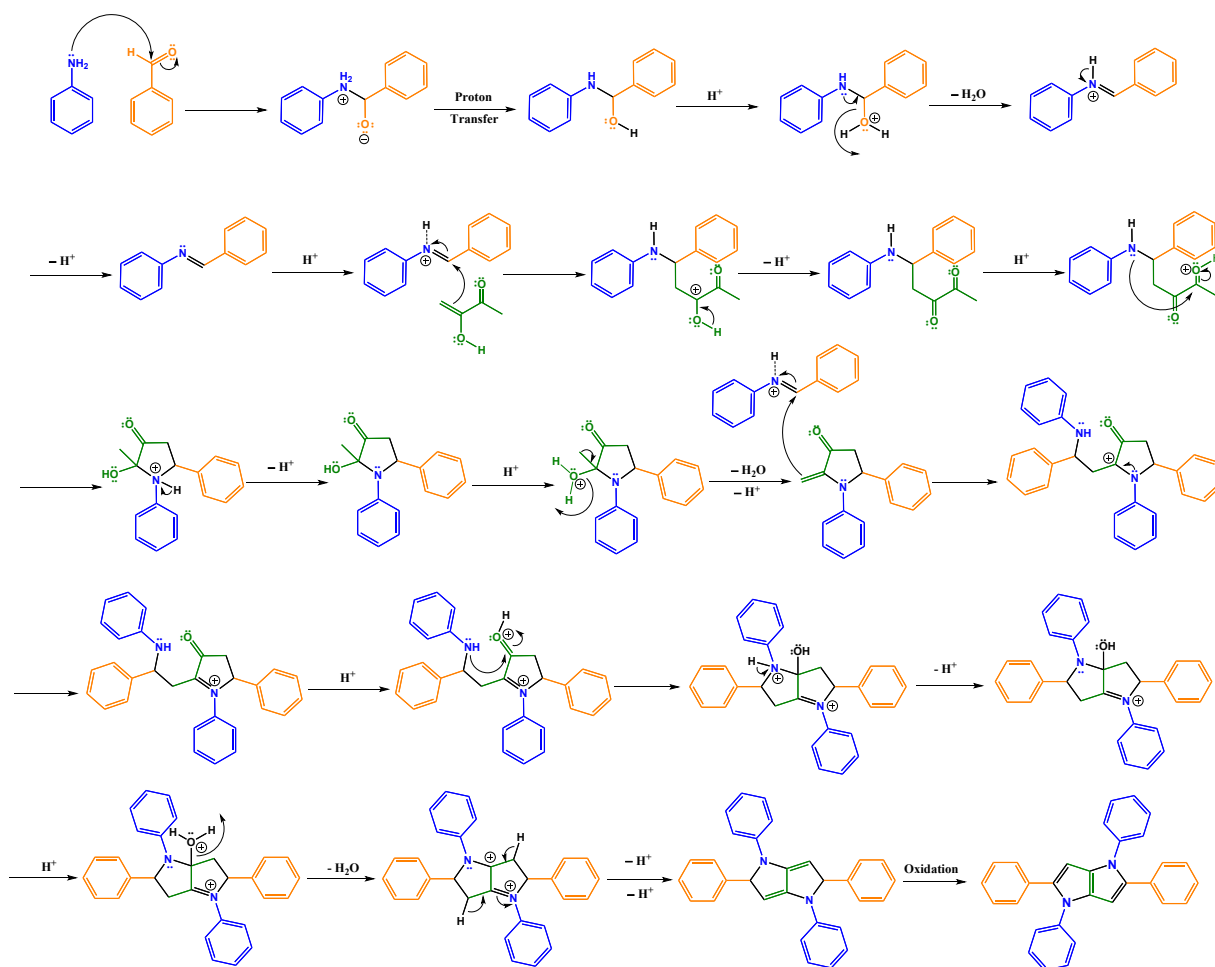


Figure S3. ^{13}C NMR spectrum of TPPy.

Mechanism formation of TPPy



Scheme S2. Mechanism formation of TPPy.

Powder XRD analysis

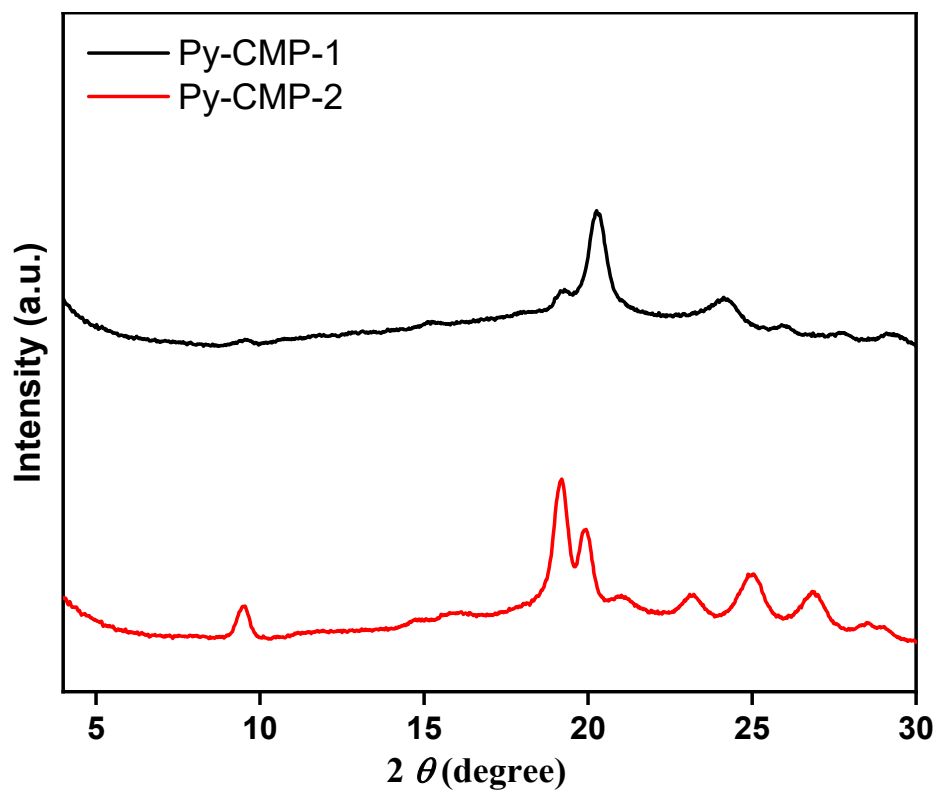


Figure S4. PXRD profiles of Py-CMP-1 and Py-CMP-2.

Transmission Electron Microscopy (TEM)

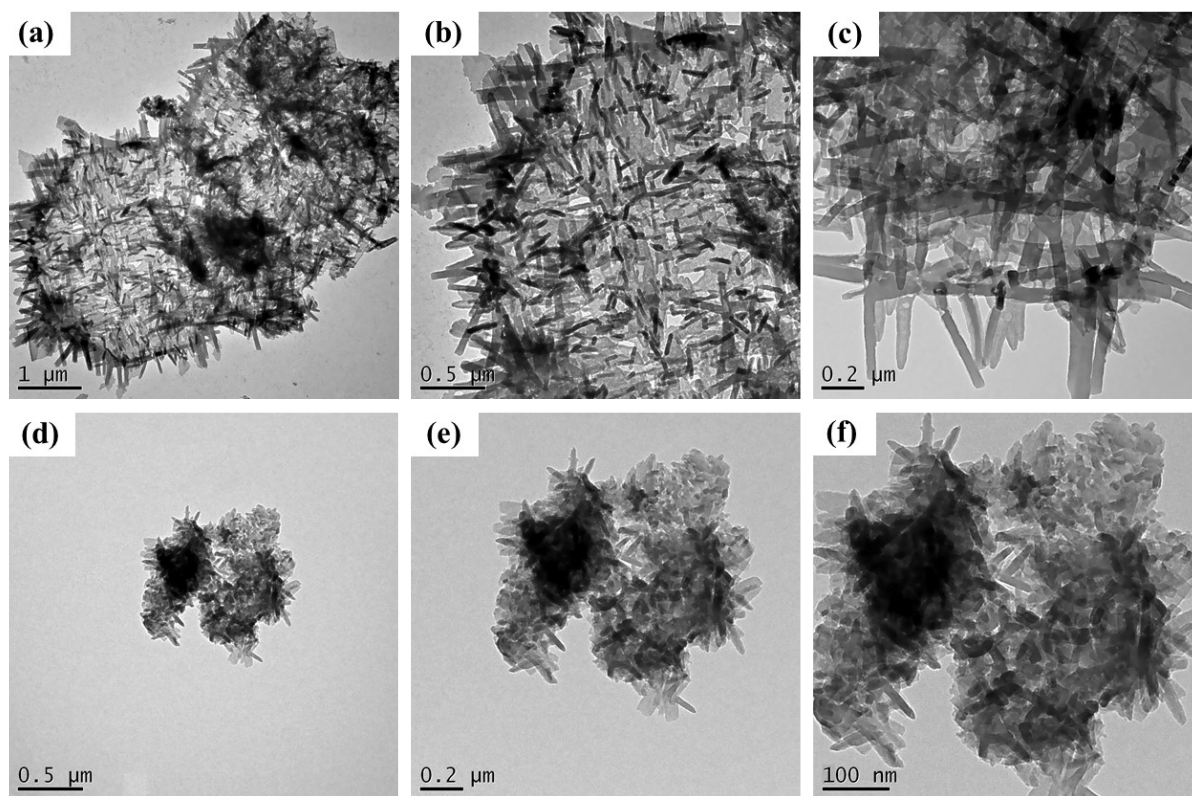


Figure S5. TEM images of (a-c) Py-CMP-1 and (c-f) Py-CMP-2 at different magnification scales.

Chemical Stability

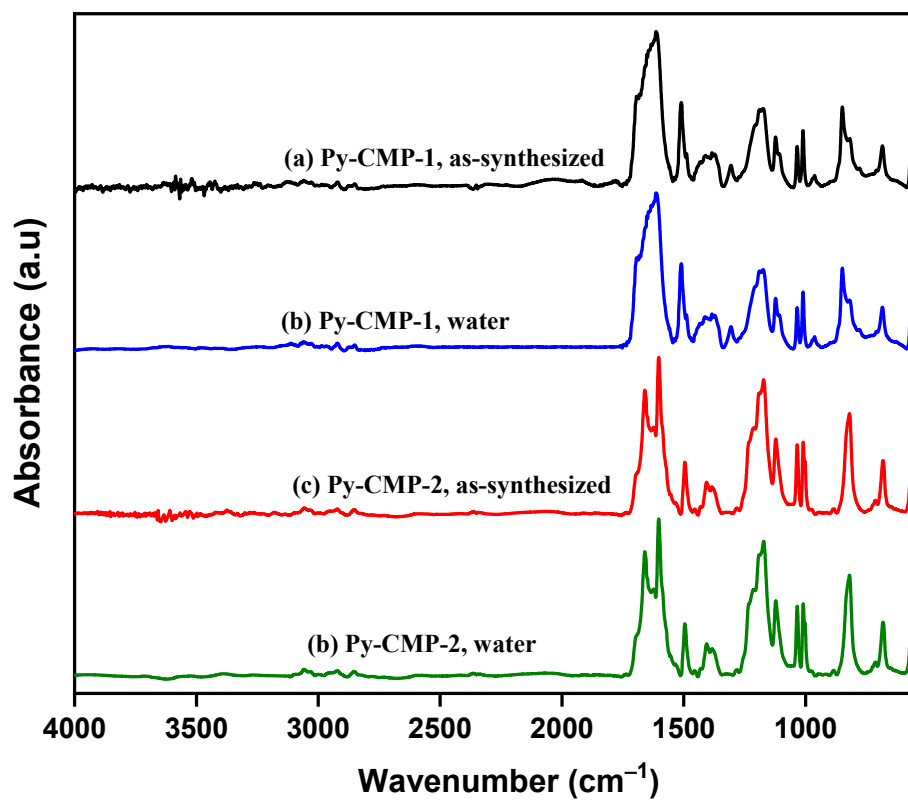


Figure S6. FTIR spectra of (a,c) Py-CMP-1 as-synthesized and (c,d) after immersing 4 days in water.

Diffuse Reflectance UV-vis Spectra

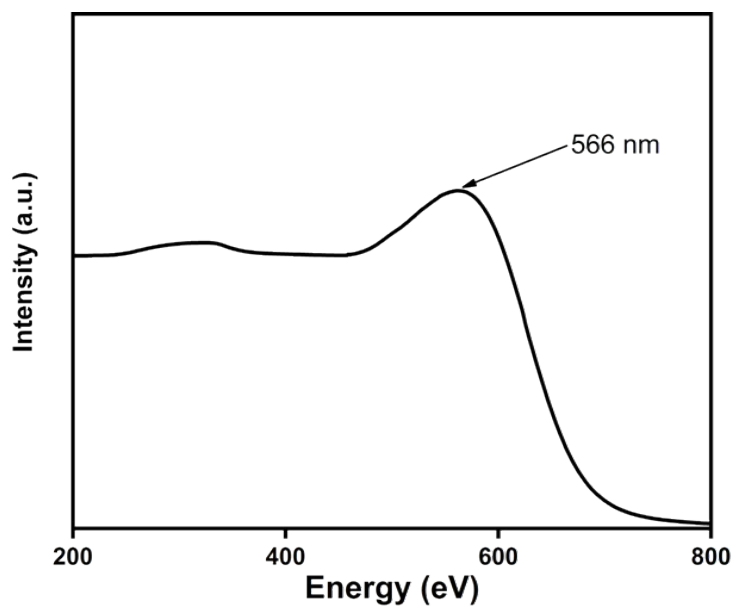


Figure S7. UV-Vis DRS spectra of Py-CMP-1.

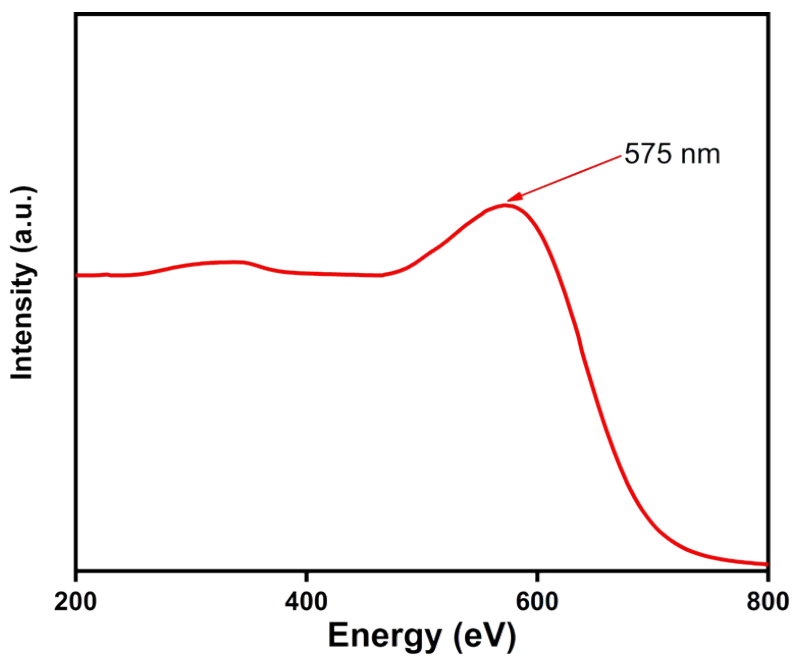


Figure S8. UV-Vis DRS spectra of Py-CMP-2.

Cyclic Voltammetry and Electronic band levels

Cyclic voltammetry (CV) measurements were carried out using Zahner Zennium 6273E workstation with three electrode configuration. The electrolyte is 0.1 M tetrabutylammonium hexafluorophosphate (TBAPF₆) using distilled acetonitrile as solvent. CHI 102 platinum working electrode (2 mm diameter) was used as the working electrode, RE-7 Ag/AgCl (0.1 M Ag/Ag⁺ acetonitrile solution) reference electrode was used as the reference electrode and platinum wire electrode was used as the counter electrode. 5 mg of the catalyst was mixed with isopropyl alcohol mixture (10 mL), subsequently added 25 μL of 5 wt. % Nafion to it and sonicated in a bath sonicator for 1h. 10 μL of the catalyst ink was drop casted on the working carbon electrode surface and air dried overnight.

For optical band gaps for Py-CMP-1 and Py-CMP-2, the Tauc plots were performed according to the Kubelka–Munk function.^{S1,S2} The following equation is used to calculate optical band gap using absorption spectra:

$$\alpha h\nu = A(h\nu - E_g)^{n/2}$$

Where α is the optical absorption coefficient, h is the Planck constant, ν is the light frequency, E_g is the optical band gap, and A is the a cinstant depending on electron-hole mobility. The value of n is 1. Then, The E_g of the samples could well be determined from a plot of $(\alpha h\nu)^{1/2}$ versus energy ($h\nu$), and its value can be derived from the intercept of the tangent to the X axis.

For the energy levels of the highest occupied molecular orbitals (HOMOs) of the as-prepared Py-CMPs, a photoelectron spectrometer was used.^{S3-S5} The photoelectric effect is used in the photoelectron spectrometer method, which measures the photocurrent while irradiating the sample with monochromatic light of varying energy. There is a linear relationship between the n th power of photoelectron emission yield ($Y^{1/2}$) and the excitation photon energy (E) for semiconductors.^{S6-S8} The common value of n photoelectron spectrometer is 0.5. This photoemission process is given by the following

$$Y^{1/2} \propto (E - HOMO)$$

Therefore, to determine the HOMO levels of our Py-CMPs, we plotted the squar root of the photoelectron emission yield versus the excitation photon energy. The threshold energy is equal the HOMO energy of the Py-CMPs.

Table S1. Absorption maxima and energy levels of the Py-CMPs.

Photocatalyst	λ_{\max} [nm] ^[a]	E_g [eV] ^[b]	LUMO[eV] ^[c]	HOMO[eV] ^[d]	LUMO[eV] ^[e]
Py-CMP-1	566	1.80	-3.78	-5.68	-3.88
Py-CMP-2	575	1.76	-3.74	-5.62	-3.86

[a] Absorption was determined in solid state using reflectance mode; [b] Determined by the onset of UV-vis absorption; [c] Measured in acetonitrile/TBAPF₆ (0.1 M) solution, CHI 102 platinum working electrode was used as the working electrode, platinum wire as the counter electrode, Ag/AgCl reference electrode as the reference electrode, and Fc/Fc⁺ as an internal standard. Estimated vs vacuum level from LUMO = -[E_{red}-E[FC/FC⁺] + 4.8] eV; [d] Calculated from the photoelectron spectrometer; [e] Calculated from LUMO = HOMO^d - E_g.

Photocurrent Measurement

The photocurrent response measurements were performed on a Zahner Zennium 6273E workstation equipped with visible-light irradiation with a conventional three-electrode cell including a Pt wire counter electrode, Ag/AgCl as reference electrode (3 M NaCl) and an indium tin oxide (ITO) glass as working electrode. About 5 mg of Py-CMPs were dispersed into an acetonitrile solution (1 mL) with 30 μ L Nifion and sonicate for 30 min to obtain a slurry mixture. After that, 200 μ L of as-prepared slurry was spread onto ITO glass with an active area of 6.875 cm². Here, 0.5 M Na₂SO₄ aqueous solution was prepared as electrolyte. 0.8 V constant potential was applied with the 20 s light on-off after a certain time interval to record the photo and dark current. A 300 W Xe lamp with a visible-light band-pass filter ($\lambda > 450$ nm) was employed as the excitation light source.

Reference:

- S1. C. Yang, Z. Cheng, G. Divitini, C. Qian, B. Hou, Y. Liao, *J. Mater. Chem. A*, 2021, **9**, 19894–19900.
- S2. Sivakarthik, V. Thangara, M. Parthibavarman, *J. Mater. Sci.: Mater. Electron.*, 2017, **28**, 5990–5996.
- S3. Riken Keiki Co., Tokyo, model AC-3, <http://www.rikenkeiki.co.jp/english/>.
- S4. Y. Guo, W. Sato, K. Inoue, W. Zhang, G. Yu, E. Nakamura, *J. Mater. Chem. A*, 2016, **4**, 18852–18856.
- S5. M. Onoda, K. Tada, H. Nakayama, *J. Appl. Phys.*, 1999, **86**, 2110.
- S6. J. Jasieniak, M. Califano, S. E. Watkins, *ACS Nano*, 2011, **5**, 5888–5920.
- S7. T. Kameyama, T. Takahashi, T. Machida, Y. Kamiya, T. Yamamoto, S. Kuwabata, T. Torimoto, *J. Phys. Chem. C*, 2015, **119**, 24740–24749.
- S8. S. Lacher, Y. Matsuo, E. Nakamura, *J. Am. Chem. Soc.*, 2011, **133**, 16997–17004.

Dye adsorption Experiments

The performance of the Py-CMP-1 and Py-CMP-2 for dye removal from water was demonstrated using RhB organic dye. In this experiment, a weight of 4 mg of Py-CMP-1 and Py-CMP-2 was added to an aqueous solution of RhB (10 mL, 25 mg L⁻¹) in a glass vial with stirring for (0, 5, 10, 15, 30, 60, or 90 min) at a rate of 800 rpm. Centrifugation (6000 rpm, 10 min) was then carried out to isolate the supernatant, then the UV–Vis spectrum of the isolated supernatant was recorded.

Different concentrations of dye solution (from 12.5 to 200 mg L⁻¹) were used in order to obtain adsorption isothermal curves. At every experiment, a specific amount of Py-CMP-1 and Py-CMP-2 (2 mg) was added to the previous prepared RhB aqueous solutions (10 mL) in a glass vial with stirring at a rate of 800 rpm for a period of 24 h. The clear dye solution was separated from mother liquor using centrifugation and then, its UV–Vis spectrum was measured. The equilibrium adsorption of dye per unit mass of the adsorbent, Q_e (mg g⁻¹),^{S9} was estimated as follows:

$$Q_e = (C_0 - C_e) \times V \times m^{-1}$$

Where C_0 (mg L⁻¹) is the initial dye concentration in the liquid phase, C_e (mg L⁻¹) is the equilibrium dye concentration in the liquid phase, V (L) is volume of dye solution, and m (mg) is the mass of CMP.

The adsorption isotherms were fitted using the Langmuir isothermal model (linear form) which presented as follows:

$$\frac{C_e}{Q_e} = \frac{1}{K_L Q_m} + \frac{C_e}{Q_m}$$

where K_L (L mg⁻¹) is the Langmuir constant; and Q_m (mg g⁻¹) is the maximum equilibrium adsorption of dye per unit mass of the adsorbent.

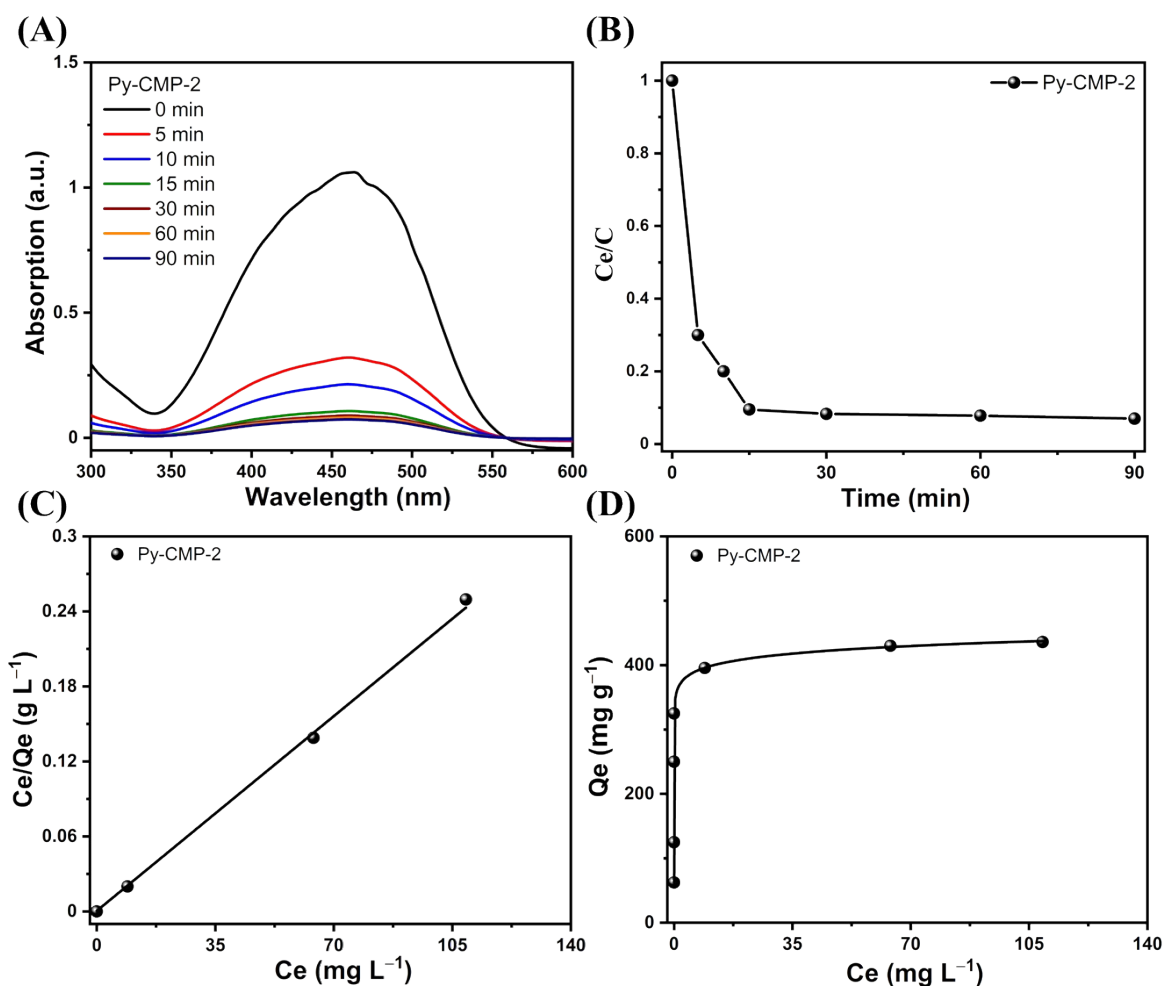


Figure S9. (A) UV–Vis spectra of an aqueous organic MO solution (25 mg L^{-1}) recorded at various time intervals after the addition of Py-CMP-2. (B) Rates of adsorption of MO from an aqueous solution (25 mg L^{-1}) onto Py-CMP-2, measured at various periods of time. (C) Langmuir isothermal model and (D) adsorption isothermal curve for the adsorption of MO onto Py-CMP-2.

Table S2. Fitted parameters for the adsorptions of RhB on the Py-CMPs, calculated using the Langmuir adsorption isothermal model.

Photocatalyst	$Q_m \text{ (mg g}^{-1}\text{)}$	K_L	R_L^2
Py-CMP-1	235	0.852	0.9998
Py-CMP-2	475	0.571	0.9991

Table S3. Maximum adsorption capacities of RhB on the Py-CMPs, compared with those of other reported materials.

Adsorbent	Dye	Q_m (mg g ⁻¹)	BET(m ² g ⁻¹)	Amount/dye conc.	Ref.
Graphene sponge	RhB	72	150	2 mg ml ⁻¹ /95 mg l ⁻¹	S10
Nanoporous PDVB-VI-0.2	RhB	260	737	0.5 mg ml ⁻¹ /50 mg l ⁻¹	S11
S1	RhB	200	48.6	0.08 mg ml ⁻¹ /40 mg l ⁻¹	S12
activated carbon (OAC)	RhB	312-409	543	0.1-1.5 mg ml ⁻¹ /100-450 mg l ⁻¹	S13
Mesoporous carbon (ST-A)	RhB	83-100	670	0.03-0.7 mg ml ⁻¹ /30-310 mg l ⁻¹	S14
N-doped mesoporous gyroid carbon	RhB	204	491	0.5 mg ml ⁻¹ /12.5-150 mg l ⁻¹	S15
CMP-YA	RhB	535	1410	0.2 mg ml ⁻¹ /25 mg l ⁻¹	S16
Py-BF-CMP	RhB	1905	1306	0.2 mg ml ⁻¹ /25 mg l ⁻¹	S17
TPE-BF-CMP	RhB	1024	777	0.2 mg ml ⁻¹ /25 mg l ⁻¹	S17
TPA-BF-CMP	RhB	926	590	0.2 mg ml ⁻¹ /25 mg l ⁻¹	S17
Ttba-TPDA-COF	RhB	833	726	0.5 mg ml ⁻¹ /20-800 mg l ⁻¹	S18
CuP-DMNDA-COF/Fe	RhB	378-429	273	0.25 mg ml ⁻¹ /16 mg l ⁻¹	S19
BIPE-BIPE	RhB	352	918	0.4 mg ml ⁻¹ /25 mg l ⁻¹	S20
BIPE-Py	RhB	1027	1400	0.4 mg ml ⁻¹ /25 mg l ⁻¹	S20
BIPE-TPT	RhB	739	903	0.4 mg ml ⁻¹ /25 mg l ⁻¹	S20
Py-CMP-1	RhB	235	206	0.4 mg ml ⁻¹ /25 mg l ⁻¹	This work
Py-CMP-2	RhB	475	311	0.4 mg ml ⁻¹ /25 mg l ⁻¹	This work

Reference:

- S9. M. B. Zakaria, A. A. Belik, C. H. Liu, H. Y. Hsieh, Y. T. Liao, V. Malgras, Y. Yamauchi and K. C. W. Wu, *Chem. Asian J.*, 2015, **10**, 1457–1462.
- S10. J. Zhao, W. Ren and H. M. Cheng, *J. Mater. Chem.*, 2012, **22**, 20197-20202.
- S11. Y. Han, W. Li, J. Zhang, H. Meng, Y. Xu and X. Zhang, *RSC Adv.*, 2015, **5**, 104915-104922.
- S12. S. Wang, B. Yang and Y. Liu, *J. Colloid Interface Sci.*, 2017, **507**, 225-233.
- S13. O. Üner, Ü. Geçgel, H. Kolancılar and Y. Bayrak, *Chem. Eng. Commun.*, 2017, **204**, 772-783.
- S14. K. Jedynak, D. Wideł and N. Redzia, *Colloids Interfaces*, 2019, **3**, 30.
- S15. A. F. M. EL-Mahdy, T. E. Liu and S. W. Kuo, *J. Hazard. Mater.*, 2020, **391**, 122163.
- S16. Y. Yuan, H. Huang, L. Chen and Y. Chen, *Macromolecules*, 2017, **50**, 4993–5003.
- S17. B. Wang, Z. Xie, Y. Li, Z. Yang and L. Chen, *Macromolecules*, 2018, **51**, 3443-3449.
- S18. T. Xu, S. An, C. Peng, J. Hu and H. Liu, *Ind. Eng. Chem. Res.*, 2020, **59**, 8315-8322.
- S19. Y. Hou, X. Zhang, C. Wang, D. Qi, Y. Gu, Z. Wang and J. Jiang, *New J. Chem.*, 2017, **41**, 6145-6151.
- S20. A. F. Saber and A. F. M. EL-Mahdy, *New J. Chem.* 2021, **45**, 21834-21843.

Photodegradation Experiments

To avoid RhB decomposition due to UV irradiation, a 450 nm optical filter was placed in front of the 300 W xenon lamp light source to shut off UV light and ensure that photocatalytic degradation is driven by visible light and under at ambient temperature and pressure. The blank experiment without adding Py-CMPs was conducted with 60 mL of RhB solution (10 mg L^{-1}) and irradiated with visible light for 180 min. The distance between the liquid level and the filter is fixed at 5 cm.

In a typical Photodegradation experiment, a weight of 6 mg of Py-CMP-1 and Py-CMP-2 was added to an aqueous solution of RhB (60 mL, 20 mg L^{-1}) in a glass In a 100 mL sandwich beaker and magnetically stirred with the rate of 800 rpm for 90 min in the dark for reaching the saturation of adsorption of dye. The entire mixture was kept at room temperature by using circulating water. The entire mixture was performed under visible light irradiation during the course of the photocatalytic experiment for 330 min for Py-CMP-1 and 310 min for Py-CMP-2. An aliquot of the reaction mixture (2 mL) was taken by a pipette every 30 min to monitor the degradation process, for which the catalyst was emoved through centrifugation (6000 rpm, 10 min). Then, the UV–Vis spectrum of the isolated supernatant was recorded. The degradation efficiency (%) was calculated from equation listed below:

$$\text{Degradation efficiency (\%)} = \frac{C_0 - C_e}{C_0} \times 100$$

Where C_0 (mg L^{-1}) is the initial dye concentration in the liquid phase and C_e (mg L^{-1}) is the equilibrium dye concentration in the liquid phase at $t = 0$ and t minutes of photocatalytic reaction.

For reusability of Py-CMP-1 and Py-CMP-2 for organic RhB dye degradation, the solutions were filtered to recover the Py-CMP-1 and Py-CMP-2 catalysts, and to guarantee that the adsorbed dyes were removed, the catalysts were washed with a significant amount of water and ethanol. The recovered catalysts were then activated under vacuum at 80°C for 4 hours and FTIR analyzed before being utilized in the next cycle. Each cycle experiment was carried out under the identical conditions to verify the correctness of the results. The radical scavenger experiments were performed using sodium azide (32 mg mL^{-1}), benzoquinone (54 mg mL^{-1}), isopropanol alcohol (30 mL mL^{-1}) and ethylenediaminetetraacetic acid disodium salt (186 mg mL^{-1}).

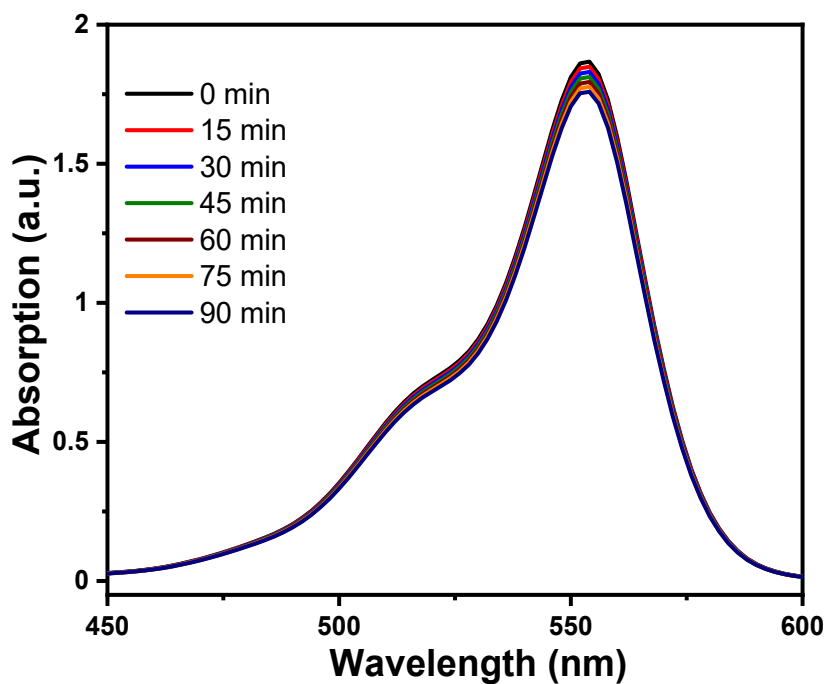


Figure S10. UV-vis monitoring of the control experiment of RhB (20 mg L^{-1}) upon visible light irradiation ($\lambda > 450 \text{ nm}$) for 90 min without catalyst.

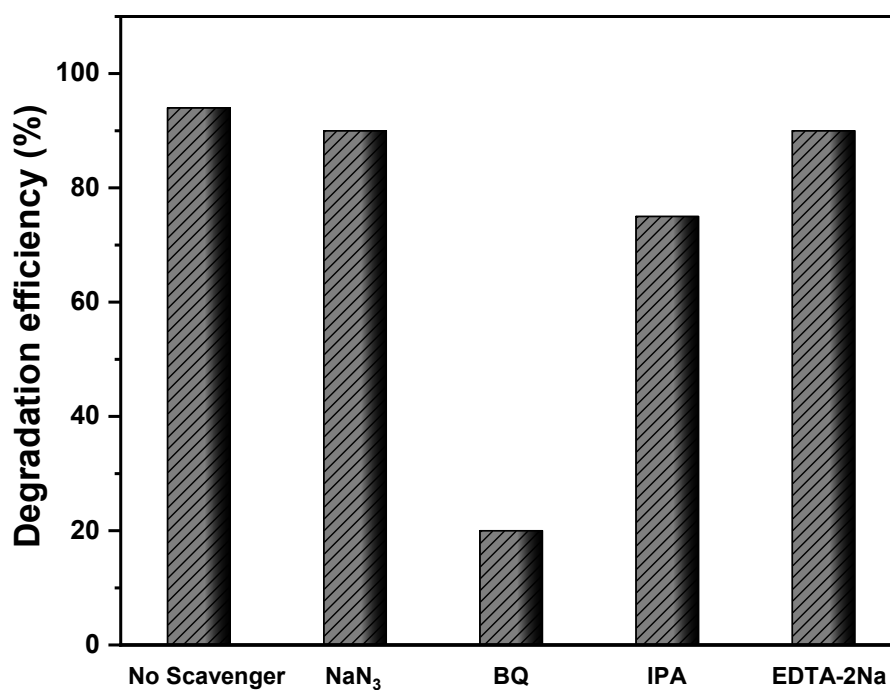


Figure S11. Effect of different scavengers, NaN_3 , BQ, IPA and EDTA-2Na on the photocatalytic degradation of RhB (20 mg L^{-1}) by Py-CMP-2 under visible light irradiation ($\lambda > 450 \text{ nm}$) for 90 min.

Table S4. Photodegradation performance of RhB on the Py-CMPs, compared with those of other reported materials.

Catalyst	Preparation method	Catalyst amount (mg)	Dye RhB solution	Degradation time (min)	Degradation efficiency (%)	Ref.
Py-BF-CMP	Pd(PPh ₃) ₄ ,DMF, 150 °C, 36 h	10	75 mg L ⁻¹ , 50 mL	90	<90	S17
TPE-BF-CMP	Pd(PPh ₃) ₄ ,DMF, 150 °C, 36 h	10	55 mg L ⁻¹ , 50 mL	90	~90	S17
TPA-BF-CMP	Pd(PPh ₃) ₄ ,DMF, 150 °C, 36 h	10	40 mg L ⁻¹ , 50 mL	90	~90	S17
α-ZnPc-CMP	Polyphosphoric acid, 80 °C, 8 h	10	4.42 mg L ⁻¹ , 40 mL	90	~56	S21
α-ZnPc-CMP /H ₂ O ₂	Polyphosphoric acid, 80 °C, 8 h	10	4.42 mg L ⁻¹ , 40 mL	90	~90	S21
β-ZnPc-CMP	Polyphosphoric acid, 80 °C, 8 h	10	4.42 mg L ⁻¹ , 40 mL	90	~50	S21
β-ZnPc-CMP /H ₂ O ₂	Polyphosphoric acid, 80 °C, 8 h	10	4.42 mg L ⁻¹ , 40 mL	90	~80	S21
B-FL ₃ -a CMP	Pd(PPh ₃) ₄ ,CuI, TEA,Toluene, 80 °C, overnight	1 mg L ⁻¹	10 mg L ⁻¹ , 20 mL	30	~10	S22
B-BPh ₃ -a CMP	Pd(PPh ₃) ₄ ,CuI, TEA,Toluene, 80 °C, overnight	1 mg L ⁻¹	10 mg L ⁻¹ , 20 mL	30	~10	S22
B-BT ₃ -a CMP	Pd(PPh ₃) ₄ ,CuI, TEA,Toluene, 80 °C, overnight	1 mg L ⁻¹	10 mg L ⁻¹ , 20 mL	30	50	S22
B-FL ₃ -b CMP	Pd(PPh ₃) ₄ ,CuI, TEA,Toluene, 80 °C, overnight	1 mg L ⁻¹	10 mg L ⁻¹ , 20 mL	30	Non	S22
B-BPh ₃ -b CMP	Pd(PPh ₃) ₄ ,CuI, TEA,Toluene, 80 °C, overnight	1 mg L ⁻¹	10 mg L ⁻¹ , 20 mL	30	~37.5	S22
B-BT ₃ -b CMP	Pd(PPh ₃) ₄ ,CuI, TEA,Toluene, 80 °C, overnight	1 mg L ⁻¹	10 mg L ⁻¹ , 20 mL	30	80	S22
Bn-Anderson-CMP	PdCl ₂ (PhCN) ₂ , tri(o-tolyl)phosphine, CuI, DMF, 100 °C, 72 h.	40	10 mg L ⁻¹ , 40 mL	30	81	S23
Th-Anderson-CMP	PdCl ₂ (PhCN) ₂ , tri(o-tolyl)phosphine, CuI, DMF, 100 °C, 72 h.	40	10 mg L ⁻¹ , 40 mL	30	~60	S23
MoS ₂ /COF	MoS ₂ , COF, and thiourea, Autoclave, 1200 °C, 12 h.	10	20 mg L ⁻¹ , 20 mL	30	98	S24
Py-CMP-1	AcOH/95 °C, 1 h	6	20 mg L ⁻¹ , 60 mL	90	16.2	This work
Py-CMP-1	AcOH/95 °C, 1 h	6	20 mg L ⁻¹ , 60 mL	90	95.77	This work

Reference:

- S21. L. Cai, Y. Li, Y. Li, H. Wang, Y. Yu, Y. Liu, and Q. Duan, *J. Hazard. Mater.*, 2018, **348**, 47–55.
- S22. B. C. Ma, S. Ghasimi, K. Landfester, F. Vilela, and K. A. I. Zhang, *J. Mater. Chem. A*, 2015,**3**, 16064–16071.
- S23. Y. Li, M. Liu, and L. Chen, *J. Mater. Chem. A*, 2017,**5**, 13757–13762.
- S24. K. K. Khaing, D. Yin, Y. Ouyang, S. Xiao, B. Liu, L. Deng, L. Li, X. Guo, J. Wang, J. Liu, and Y. Zhang, *Inorg. Chem.*, 2020, **59**, 6942–6952.